Applied and Environmental Microbiology

Simultaneous Quantification of Active Carbon- and Nitrogen-Fixing Communities and Estimation of Fixation Rates Using Fluorescence *In Situ* Hybridization and Flow Cytometry

Allison S. McInnes, Alicia K. Shepard, Eric J. Raes, Anya M. Waite and Antonietta Quigg

Appl. Environ. Microbiol. **2014, 80(21):6750. DOI: 10.1128/AEM.01962-14.**
Published Ahead of Print 29 August 2014.

AEM
Journals.ASM.org

Simultaneous Quantification of Active Carbon- and Nitrogen-Fixing Communities and Estimation of Fixation Rates Using Fluorescence *In Situ* Hybridization and Flow Cytometry

Allison S. McInnes,[a]* Alicia K. Shepard,[a] Eric J. Raes,[b] Anya M. Waite,[b,c]* Antonietta Quigg[a,d]

Department of Oceanography, Texas A&M University, College Station, Texas, USA[a]; The Oceans Institute, University of Western Australia, Crawley, WA, Australia[b]; The School of Civil, Environmental and Mining Engineering, University of Western Australia, Crawley, Western Australia, Australia[c]; Department of Marine Biology, Texas A&M University at Galveston, Galveston, Texas, USA[d]

Understanding the interconnectivity of oceanic carbon and nitrogen cycles, specifically carbon and nitrogen fixation, is essential in elucidating the fate and distribution of carbon in the ocean. Traditional techniques measure either organism abundance or biochemical rates. As such, measurements are performed on separate samples and on different time scales. Here, we developed a method to simultaneously quantify organisms while estimating rates of fixation across time and space for both carbon and nitrogen. Tyramide signal amplification fluorescence *in situ* hybridization (TSA-FISH) of mRNA for functionally specific oligonucleotide probes for *rbcL* (ribulose-1,5-bisphosphate carboxylase/oxygenase; carbon fixation) and *nifH* (nitrogenase; nitrogen fixation) was combined with flow cytometry to measure abundance and estimate activity. Cultured samples representing a diversity of phytoplankton (cyanobacteria, coccolithophores, chlorophytes, diatoms, and dinoflagellates), as well as environmental samples from the open ocean (Gulf of Mexico, USA, and southeastern Indian Ocean, Australia) and an estuary (Galveston Bay, Texas, USA), were successfully hybridized. Strong correlations between positively tagged community abundance and $^{14}C/^{15}N$ measurements are presented. We propose that these methods can be used to estimate carbon and nitrogen fixation in environmental communities. The utilization of mRNA TSA-FISH to detect multiple active microbial functions within the same sample will offer increased understanding of important biogeochemical cycles in the ocean.

Carbon is the biogeochemical currency of the ocean; its importance is exemplified in measuring either carbon dioxide sequestration (about half of anthropogenic CO_2 is sequestered by the oceans [1, 2, 64]) or potential fisheries yields (average catch of 68 Mt yr^{-1}, equating to primary production of 3.5 Gt C yr^{-1} [3]). Primary production converts atmospheric CO_2 into organic carbon, the critical first step in the introduction of C into the food web. The determination of the fate of fixed C can be estimated by examination of the source of nitrogen (4). In recent decades, it has become increasingly clear that the primary source of new N in the oligotrophic ocean is microbially mediated biological N_2 fixation (5–7). In theory, at an ecosystem level, if accurate measurements of biological N_2 fixation can be made, C sequestration and food web production also can be estimated (8). However, disparate techniques are used for the quantification of biomass and rates. Biomass measurements for phototrophs include chlorophyll *a*, pigment analysis using high-performance liquid chromatography (9), and flow cytometry (10, 11). Methods to measure rates of primary production include light/dark bottles (12, 13), ^{14}C uptake (14), stable isotopes of oxygen (^{16}O, ^{18}O, and ^{17}O) (15, 16), or fluorescence kinetics (17, 18). Similarly, for nitrogen fixation, organisms are enumerated by labeling via 4′,6-diamidino-2-phenylindole, dihydrochloride, and other nucleic acid stains, while the determination of the rates of targeted processes is executed via acetylene reduction reactions (65) or $^{15}N_2$ uptake (20–22).

Because quantification of different carbon- or nitrogen-fixing populations and estimates of their respective rates have used fundamentally different techniques, the understanding of the connectivity between these two cycles necessarily is replete with assumptions. To improve our understanding, microbial biologists need not only to determine the composition of the microbial community (DNA) but also to include process measurements, including activity (rRNA) and, recently, specific activity (mRNA) within these populations. Fluorescence *in situ* hybridization (FISH) has been employed extensively to determine abundance and general activity (using rRNA probes) of prokaryotes in aquatic environments (23). Transcript abundance (quantitative PCR [qPCR] of mRNA) of the carbon-fixing enzyme ribulose-1,5-bisphosphate carboxylase/oxygenase (RuBisCO) (24–26) and the nitrogen-fixing enzyme nitrogenase (27) correlate with their respective rate measurements. mRNA FISH is a tool capable of community quantification while simultaneously quantifying the number of organisms performing a specific function (28). Due to the low abundance of target sequences (mRNA ≪ rRNA) (26), the amplification of the signal using tyramide signal amplification (TSA) is necessary. Most studies have been limited to very specific groups (29, 30). This study targeted processes that span taxonomic and

Received 13 June 2014 Accepted 21 August 2014
Published ahead of print 29 August 2014
Editor: J. E. Kostka
Address correspondence to Allison S. McInnes, allison.mcinnes@uwa.edu.au.
* Present address: Allison S. McInnes, The Oceans Institute, University of Western Australia, Crawley, WA, Australia; Anya M. Waite, Alfred-Wegener-Institut Helmholtz-Zentrum für Polar-und Meeresforschung, Bremerhaven, Germany.
Supplemental material for this article may be found at http://dx.doi.org/10.1128/AEM.01962-14.

doi:10.1128/AEM.01962-14
The authors have paid a fee to allow immediate free access to this article.

genetic variability. By simultaneously incorporating universal oligonucleotide probes complementary to multiple functions actively expressed in the sample population, we can begin to understand the connectivity of carbon and nitrogen fixation via direct measurement.

The aim of this study was to develop an inclusive method employing TSA-FISH with general oligonucleotide probes complementary to *rbcL* (codes for the large subunit of RuBisCO; carbon fixation) and *nifH* (catalytic subunit of dinitrogenase reductase; nitrogen fixation) mRNA transcripts, allowing quantification of C- and N_2-fixing communities and simultaneous estimation of C and N_2 fixation rates within those communities. The application of this method reduces the number of assumptions and allows a more direct understanding of the connectivity of these two dynamic cycles.

MATERIALS AND METHODS

Probe design. In this study, our aim was to target C and N_2 fixation across the entire community rather than tagging a unique species. This necessitated first finding a conserved target region in the gene sequences across a diversity of organisms and then allowing enough generality in hybridization optimization to tag all functional representatives. We addressed the first issue during probe design (see Tables S1 and S2 in the supplemental material). We used data from GenBank (accessed January 2010; http://www.ncbi.nlm.nih.gov/nucleotide/) to compile sequences. For *rbcL*, we compiled 113 sequences, including 7 phyla representing 17 orders and 26 genera. For *nifH*, we compiled 124 sequences, including 4 phyla representing 15 orders and 37 genera. Multiple sequences were selected for many species to include interspecies variability as well as between-group variability. Sequences were compiled covering all major taxa (cyanobacteria, diatom, dinoflagellates, haptophytes, and green algae, among others, for *rbcL* and from the four major *nifH* clusters described in reference 36) so that the probes would be as near to universal as possible at the time of design. These were aligned using MEGA5/ClustalW (gap opening penalty of 15, gap extension penalty of 6.6 [http://www.megasoftware.net/]). The most conserved region was chosen and further analyzed using OligoCalc (v3.26 [http://www.basic.northwestern.edu/biotools/OligoCalc.html]) to ensure no hairpin formation potential, 3′ complementarity, or self-annealing. Comparisons of these probe sequences were performed against the GenBank database to verify specificity to primary producers and nitrogen-fixing organisms. NON338, a sequence commonly employed as a negative control, was used in this study (29, 37).

To eliminate background fluorescence from nonspecific binding of the amplification reagent used in visualization, horseradish peroxidase was directly attached (38) to the 5′ end of the oligonucleotide probes (reverse complement of the target sequence) (see Tables S1 and S2 in the supplemental material) (Life Technologies Invitrogen custom oligonucleotide probes). Because we tagged both prokaryotes and eukaryotes, a traditional positive control was not used. Instead, we verified target presence with SYBR green I nucleic acid stain (1:10,000; Molecular Probes). After the initial determination of accurate *rbcL* probe hybridization to *Synechococcus* sp. (data not shown), this culture and probe were run as a positive control, verifying chemical and probe functionality.

Maintenance and collection of laboratory cultures. In order to ensure accuracy while maintaining generality, *rbcL* probe specificity was determined using a diversity of cultured phytoplankton, including cyanobacteria (*Synechococcus* sp.), a dinoflagellate (*Thoracosphaera heimii*), diatoms (*Thalassiosira oceanica* and *Amphora coffeaeiformis*), a coccolithophore (*Emiliana huxleyi*), and a green algae (*Dunaliella tertiolecta*) (see Table S3 in the supplemental material). Cultures were grown at optimal temperatures according to the Provasoli-Guillard National Center for Culture of Marine Phytoplankton in f/2 media (39) on a 12-h light/12-h dark cycle at 19°C or 24°C and 130 to 150 μmol photons m^{-2} s^{-1}. Media recipes on the culture collection website were followed, with Gulf of Mexico seawater used as the base for the f/2 media (39). The bacterium *Escherichia coli*, grown in LB broth (LB broth base tablets; 50 ml; Tru measure; L7275-100TAB; Sigma-Aldrich) at 37°C and was used as a negative control. Samples were preserved with molecular-grade paraformaldehyde (PFA; 4× final concentration) overnight at 4°C (34). Cells then were collected via centrifugation (17,000 × *g*, 5 min) and PFA was removed; cells were resuspended in absolute ethanol (EtOH) and stored at −80°C.

Collection of environmental samples. Environmental samples were collected to test hybridization of probes for both *rbcL* and *nifH*. Samples were collected in the Gulf of Mexico (between 26 and 27°N, 86 and 92°W; June 2011) and the southeastern Indian Ocean (between 13 and 32°S, 100 and 125°W, August-September 2012) where biological nitrogen fixation has been documented (see Fig. S1 in the supplemental material) (35, 40). Samples also were collected from Galveston Bay (Texas, USA; 29.34°N, 94.50°W), representing an environment where biological nitrogen fixation is unlikely (see Fig. S1). Water samples were concentrated using gentle vacuum filtration (<2 mm Hg) onto a Whatman Nuclepore polycarbonate track-etched membrane 0.2-μm filter (25 mm; noting volume for concentration calculations after analysis). Membrane filters were placed in a microcentrifuge tube with phosphate-buffered saline (PBS; autoclaved and filtered with 0.2-μm-pore-size filters; 750 μl), and cells were vortexed off the filters so they could be analyzed using flow cytometry (41). Samples were preserved with molecular-grade PFA (4× final concentration) overnight at 4°C (34). Cells then were collected via centrifugation (17,000 × *g*, 5 min) and PFA was removed; cells were resuspended in absolute ethanol and stored at −80°C.

Prior to collection of environmental samples, various protocols were tested to determine the optimum concentrating procedure. Duplicate water samples were collected from Galveston Bay, and an initial chlorophyll *a* measurement was made using a Turner Instruments 10AU fluorometer. Samples then were filtered (100 ml) onto Whatman Nuclepore polycarbonate track-etched membrane 0.2-μm filters (25 mm). Reverse filtration and vortexing the filter in PBS were tested for removing the samples from filters. Reverse filtration resulted in a 70 to 77% recovery, while vortexing recovered between 95 and 99%. Vortexing in PBS then was used as the standard procedure for all environmental samples.

Method comparison. (i) ^{14}C incorporation rates over diel cycles. Carbon and nitrogen fixation rates vary on a diel cycle (20, 42). Laboratory cultures of *Synechococcus* sp., *T. heimii*, and *T. oceanica* were grown in triplicate batch cultures using the same media and growth conditions as those described above. Samples were harvested every 3 h over a 24-h cycle and processed for ^{14}C uptake using the small bottle method (43); additional aliquots were preserved for mRNA FISH at the same time. Samples were inoculated with ^{14}C sodium bicarbonate (final concentration, 1 μCi ml^{-1}) for 20 min at 16 light intensities (0 to 1,800 μmol photons m^{-2} s^{-1}) at 24°C in a photosynthetron. Triplicate blanks and total counts (to determine specific activity) were prepared. Incubations were terminated with buffered formalin (50 μl), and all samples were acidified for 24 h. Radioactivity was measured using a Beckman LS8100 scintillation counter.

To elucidate the importance of diel periodicity in C fixation, the median value for replicate samples from the TSA-FISH analysis were interpolated (linear) over the 24-h cycle. These data then were integrated over various time periods (12 h of light and the entire 24 h) to compare to standard protocols (44). The amplitude (minimum subtracted from maximum) was calculated to demonstrate the intensity of the diel variation.

(ii) N^{15} incorporation rates. Environmental samples were used solely for optimization and method comparison for *nifH* probes, because no laboratory samples were available. Samples for analysis of *nifH* mRNA expression versus $^{15}N_2$ uptake were those collected in the eastern Indian Ocean during two cruises in August and September of 2012 (see Fig. S1 in the supplemental material). Aliquots for mRNA FISH were collected every 3 h, while $^{15}N_2$ uptake measurements were made at every other time point (every 6 h) over a 24-h cycle. Direct addition of $^{15}N_2$ tracer-enriched seawater was used to estimate N_2 fixation rates (21, 45). The tracer was

TABLE 1 Steps and methods involved in optimization of FISH

Process	Method	Source or reference
Fixation	2% PFA for 30 min at RT	31, 32
	2–4% PFA for 1–24 h	33
	5–10% Formalin overnight	34
	4% PFA for 12–24 h at 4°C	This study
Storage	Collect and resuspend cells/pellets in molecular-grade 100% EtOH and store at −80°C	
Permeabilization	5 mg ml^{-1} lysozyme for 30 min at RT	31, 32
	96% EtOH	29
	7% Tween 20	
	0.1% DEPC for 12 min at RT or 0.5% SDS for 10–15 min	31
	5 mg ml^{-1} lysozyme 30 min at RT	This study
	1% SDS for 1 h at RT	
Quenching	0.1% DEPC for 12 min at RT	31, 32
	1–3% H_2O_2 for 60 min at RT	Kit
	0.1% DEPC for 12 min at RT	29
	0.01% H_2O_2 for 10 min at RT	This study
Probe concn	250 ng μl^{-1} for 24 h	31, 32
	25 ng μl^{-1} for 2.5 h	29
	50 ng μl^{-1}	33
	Probe concn vs cell concn	This study
Fluorophore concn	0.25–0.5 μg ml^{-1} for 5 min at RT	31, 32
	1:50	29
	1:100 for 5–10 min at RT	Kit
	1:100 for 30 min at RT	This study

prepared by degassing and filtering (0.2-μm Sterivex filter) YBC-II media (35, 46) and stored in 3-liter gas-tight Tedlar bags, which were then spiked with 0.8 to 1 ml $^{15}N_2$ (98 atom%; Aldrich) gas per 100 ml YBC-II media. Incubations were initiated by introducing $^{15}N_2$ tracer-enriched seawater aliquots of 2.6% of the total incubation volume. Bottles were incubated for 6 h. Experiments were stopped by collecting the suspended particles from each bottle by gentle vacuum filtration (pressure, <2 mm Hg) through a 25-mm precombusted GF/F filter, snap-frozen in liquid nitrogen, and stored at −80°C.

Filters for total N and δ-^{15}N isotope analysis were dried, acidified, and dried again overnight at 60°C. Determination of total N and δ-^{15}N was carried out using a continuous flow system consisting of a SERCON 20-22 mass spectrometer connected with an automated nitrogen carbon analyzer (Sercon, United Kingdom). Samples for natural particulate organic nitrogen (PON) were obtained by gentle vacuum filtering of 4-liter water samples onto precombusted GF/F filters. N_2 fixation rates (in nmol N $liter^{-1}$ h^{-1}) were calculated by following Dugdale and Goering (4). A detailed explanation of fixation rate calculations can be found in the Protocols for the Joint Global Ocean Flux Study (44).

Fluorescence *in situ* hybridization for flow cytometry. The hybridization and detection protocol used is based on Pernthaler and Amann (26), with some modifications (Table 1). Preserved laboratory and environmental samples were collected via centrifugation (17,000 × *g*, 5 min), and ethanol was removed. Cells were resuspended in 1× PBS (0.14 M NaCl, 2.7 mM KCl, 10.1 mM Na_2HPO_4, 1.8 mM KH_2PO_4) and centrifuged again to remove PBS (here this process is referred to as a wash/washed step). Endogenous peroxidase activity and RNAses were quenched/removed by incubation of samples in 0.1% diethylpyrocarbonate (DEPC) for 12 min at room temperature (RT) (28) followed by a wash to remove DEPC. Cells were permeabilized by incubation in 5 mg ml^{-1} lysozyme for 1 h at 35°C, followed by a wash in 1× PBS, and resuspended in 1% sodium dodecyl sulfate (SDS) for 1 h at RT (33). Postpermeabilization, the cells were incubated in 0.01% fresh H_2O_2 for 10 min at RT to quench any newly exposed peroxidases.

The specificity of the oligonucleotide probes was optimized using various formamide concentrations (47) instead of various incubation temperatures, because the horseradish peroxidase (HRP) attached to the 5′ end of the probes is unstable above 35°C (31). It should be noted that the equation used to determine the specificity of oligonucleotide probes, at its most stringent, allows for 20% mismatch (47). Cell suspensions were incubated at 35°C for 1 h in hybridization buffer containing 1 to 150 μl formamide, 30 μl 20× sodium citrate buffer (SSC; 1× SSC is 0.15 M NaCl plus 0.015 M sodium citrate; Amresco), 60 μl 10%, wt/vol, dextran sulfate, 30 μl 10%, wt/vol, blocking solution (component D; TSA kit 6, T-20916; Invitrogen), 15 μl 4 mg ml^{-1} yeast RNA, 6 μl 10 mg ml^{-1} sheared salmon sperm DNA, and 9 to 159 μl autoclaved Milli-Q water. Oligonucleotide probes were diluted in hybridization buffer and incubated at 35°C for 5 min, added to cell suspensions (final concentration, between 100 to 500 ng μl^{-1}), and incubated for 24 h at 35°C.

Cell suspensions were washed with Milli Q and then with wash buffer (0.2× SSC, 0.01%, wt/vol, SDS) at 35°C for 30 min. Probes were detected using 1:100 Alexa 647-labeled tyramide (Invitrogen TSA kit 6) in amplification buffer (0.1% blocking solution, 1% dextran sulfate, 2 M NaCl, 0.0015% fresh H_2O_2) for 30 min at RT. Cells were washed and resuspended in PBS and counterstained with 30 mM tripotassium citrate and SYBR green I nucleic acid stain (S7563; Invitrogen) at 1:10,000 and then incubated for 15 min at 35°C.

Flow cytometry. Samples were enumerated using a Beckman Coulter Gallios flow cytometer equipped with 488-nm and 638-nm lasers. Fluorescence was measured using bandpass filters corresponding to emissions for SYBR (filter 525/30) and Alexa 647 (filter 695/30). Measurements for forward scatter (FSC; roughly equivalent to size), and side scatter (SSC; indicator of granularity) also were collected (48). The concentration of 15-μm beads (6602797; Coulter CC size standard L15) was determined using a hemocytometer. These were added to samples prior to flow-cytometric analysis so that accurate sample volumes could be determined. Raw data were processed using Kaluza (v6). Cells were distinguished from other particulates using FS versus SYBR fluorescence plots. These events then were plotted using FSC versus red fluorescence (Alexa 647). Gates were drawn on control plots to ensure that unhybridized cells were not counted. These gates were transferred to sample plots (with corresponding formamide concentrations). Positive results, if present, in the negative controls were subtracted from the corresponding samples.

RESULTS

Method optimization. Successful *in situ* hybridization of mRNA depends on optimization of a number of steps, including permeabilization of cells and probe specificity, as well as minimization of background fluorescence and nonspecific binding (Table 1). The first obstacle in probing a great diversity of organisms is the accompanying variety of cell walls in the target population, making multispecies permeabilization optimization difficult. Previous studies have used minimal treatments to avoid cell loss (Table 1). These treatments were attempted initially, but binding did not occur in our samples (data not shown). When permeabilization was increased (incubated in 5 mg ml^{-1} lysozyme for 1 h at 35°C, washed, and incubated in 1% SDS for 1 h at RT), probes bound to targets. This permeabilization treatment was successful for all cultures and environmental samples, including phytoplankton with coccoliths (*E. huxleyi*), theca (*T. heimii*), or silicified frustles (*A. coffeaeiformis* and *T. oceanica*) (Fig. 1). *T. heimii* showed the greatest visual loss of the pellet; nonetheless, cells were successfully

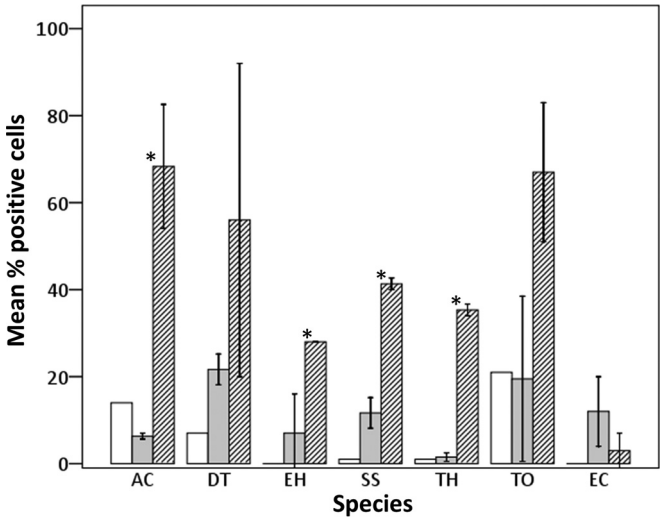

FIG 1 Hybridization of phytoplankton cultures using universal *rbcL* probe. Seven cultures were hybridized with *rbcL* and negative probes *Amphora coffeaeformis* (AC), *Dunaliella tertiolecta* (DT), *Emiliania huxleyi* (EH), *Synnechococcus* sp. (SS), *Thoracosphaera heimii* (TH), *Thalassiosira oceanica* (TO), and *Escherichia coli* (EC). Samples were run using 25% formamide for the *rbcL* (striped bars) probe and 40% formamide for the negative probe (gray bars), representing roughly equivalent specificities. Error bars (±2 standard errors) represent triplicate samples (except *D. tertiolecta*, *T. oceanica*, and *E. coli*; $n = 2$). White bars represent the intrinsic fluorescence of the samples (no probe added; controls). Some pigments remained, particularly in the diatoms. An asterisk represents samples with significant differences between positive and negative probes.

hybridized, indicating that the target cells themselves were not lost.

Minimizing background fluorescence is difficult when targeting photosynthetic organisms given the intrinsic fluorescence of the cells. Storage in absolute ethanol and subsequent permeabilization steps reduced autofluorescence. In addition, the sensitivity of the photomultiplier tubes in the flow cytometer were adjusted so that intrinsic fluorescence was accounted for with unhybridized controls. The quenching of endogenous peroxidase activity also is essential in reducing background fluorescence by limiting binding of tyramide-fluorophore to nontarget areas. The optimization of this step was essential, as the chemicals used can reduce target abundance as well as affect target integrity, and the insufficient quenching of peroxidase activity can lead to difficulties differentiating between positive target and background fluorescence (see Fig. S2 in the supplemental material). Therefore, we tested nine concentrations of H_2O_2 (0 to 1% for 10 min at RT) on *Synechococcus* sp. and found maximum differentiation of positive target to background fluorescence was achieved at 0.01% H_2O_2 (see Fig. S2). This concentration then was used for all subsequent measurements.

The separation of the microbial community from background fluorescence was accomplished using SYBR green I as a counterstain. SYBR has a strong affinity to double-stranded DNA and binds to single-stranded DNA and RNA at lower affinities (11), allowing differentiation of cells from background particulate. SYBR-positive cells were selected and subsequently analyzed for red fluorescence (Alexa 647). Red-positive events are cells that have been successfully hybridized with mRNA tags. Thus, the total microbial community (SYBR-positive cells) and the proportion showing positive target fluorescence (red-positive cells) could be quantified.

Because incubation temperature and probe concentration both affect hybridization, we also tested a matrix of formamide concentrations and probe concentrations on five different samples for *rbcL*: *Synechococcus* sp., *T. heimii*, and *T. oceanica* and water from the Gulf of Mexico (open ocean), and Galveston Bay (estuary) (see Fig. S3 in the supplemental material). Formamide concentrations of 25% yielded maximum hybridization for all of the samples, *Synechococcus* sp. (75% of total community), *T. heimii* (64% of total community), *T. oceanica* (66% of total community), Gulf of Mexico (19% of total community), and Galveston Bay (31% of total community) (see Fig. S3). The effect of probe concentration varied between samples and appeared to be primarily a function of cell concentration (data not shown). It is important to create a probe driver situation, which occurs when all target sequences are hybridized and excess probe is removed in subsequent washes (26). Hybridization specificity was purposefully less stringent here than in previous studies (26, 29, 49) in order to be general enough to capture processes across taxonomically distinct groups. Therefore, the need for negative controls was paramount. *E. coli* (negative control) did not hybridize using the methods described in this study (<5%). Further, the cultures used for verification of the positive detection using the *rbcL* probe were monospecific but not axenic, and the bacterial population present was not tagged (see Fig. S5). Additionally, negative-control probes were applied simultaneously to corresponding samples to ensure there was no nonspecific binding of the oligonucleotide probes (<3%, depending on the upon probe concentration) (see Fig. S5).

Similar matrix combinations were run for *nifH* oligonucleotide probe on samples where biological nitrogen fixation should be occurring (Gulf of Mexico) and on samples where there should be no biological nitrogen fixation (Galveston Bay) (see Fig. S4 in the supplemental material). The successful detection of active biological nitrogen fixation was achieved using a general *nifH* oligonucleotide probe (see Fig. S4) in samples from the Gulf of Mexico, where nitrogen fixation has been documented (40), but not from Galveston Bay. Galveston Bay samples showed minimal hybridization (<4%) compared to the 10 to 22% hybridization in the open-ocean Gulf of Mexico samples, indicating the specificity of the *nifH* probe to *nifH* mRNA transcripts (see Fig. S4). Hybridization was attempted using a negative-control oligonucleotide probe on all of the same treatments (variation in formamide and probe concentration) with less than 10% positive results (data not shown). Optimal results (highest positive hybridization using the *nifH* probe with minimum hybridization using the negative probe) were achieved at a 35% formamide concentration.

To account for intrinsic fluorescence and nonspecific binding of the fluorophore, control samples (with no probe added) were run for all formamide concentrations (see Fig. S5 in the supplemental material, first column). Control samples showed very limited hybridization, indicating that removal of intrinsic fluorescence and quenching of endogenous peroxidase activity were effective (see Fig. S5, column 1). Hybridization with NON338 was limited (<5%; see Fig. S5, lower 12 panels). Hybridization increased with increasing probe concentration and decreased with increasing formamide concentration (increasing specificity; see Fig. S5, upper 12 panels). The increase in fluorescence of positively

hybridized targets is sufficient to easily differentiate these from background fluorescence.

Detection of active primary producers using TSA-FISH. Cultured phytoplankton, representing a diversity of photosynthetic organisms, were successfully tagged using a general *rbcL* oligonucleotide probe (Fig. 1); this technique also was shown to be successful in samples from both coastal and open-ocean environments (see Fig. S2 in the supplemental material). The cultures were chosen to represent the diverse evolutionary history of phytoplankton (see Table S3), and all of them were small enough to be analyzed using flow cytometry (<50 μm). The variation in the total number of target cells detected (35 to 70%) (Fig. 1) may be due to differential peaks in transcription of target mRNA due to the time of day the cells were harvested (3 to 4 h after the start of the light cycle). It is known that environmental diel expression of *rbcL* peaks between 2 and 6 h after the start of the light cycle (32, 50, 51).

All differences in positive versus negative probe samples were significant ($P < 0.05$ by *t* test) (Fig. 1), except for *D. tertiolecta* ($P = 0.20$; independent-samples *t* test) and *T. oceanica* ($P = 0.06$; independent-samples *t* test). One of the triplicate samples of *D. tertiolecta* did not hybridize, yet the other two were significantly higher than the negative probe. *T. oceanica* showed a limited difference in positive versus negative hybridization. This may be due to limited signal as a result of a low number of target cells present. *E. coli* (negative control) showed no hybridization using the *rbcL* probe (Fig. 1), supporting accuracy in the specificity of the *rbcL* probe to transcripts of *rbcL* mRNA. The high degree of hybridization across a diversity of cultured organisms reveals that this technique may be successfully employed for a wide variety of samples.

Samples from estuarine (Galveston Bay) and open-ocean waters (Gulf of Mexico and the southeastern Indian Ocean) also were used to test the effectiveness of the general *rbcL* probe to quantify active primary producers in environmental samples; all environmental samples were successfully tagged (see Fig. S3 in the supplemental material). Of the total microbial plankton (0.2 to 20 μm), picoautotrophs represent ~24 to 40% in Galveston Bay, ~15 to 40% in the Gulf of Mexico (A. K. Shepard, unpublished data), and 33% in the southeastern Indian Ocean (35). Maximum percentages of the microbial population measured expressing *rbcL* were similar to the average percentages of the community: ~38% of the microbial population collected in Galveston Bay, ~10% of the microbial population from the Gulf of Mexico, and 10% (33% maximum) in the southeastern Indian Ocean (see Fig. S3). This suggests the conservation of the relative community composition in environmental samples.

Detection of active nitrogen fixers using TSA-FISH. Ten percent of the microbial population sampled in the Gulf of Mexico hybridized using the *nifH* probe. The enumeration of *nifH* expression in the Indian Ocean was 10,500 cells ml^{-1} (19% of the total community) with an average of 600 cells ml^{-1} (7% of the total community). The diversity and presence of *nifH* gene expression in environmental samples have been reported for environments around the world (36, 52). However, reported proportions of diazotrophic microbial community and abundance measurements are limited. Unicellular cyanobacteria expressing *nifH* genes can represent up to 10% of the microbial community composition (53), but this number does not account for potential heterotrophic nitrogen fixers. Our method now makes the generation of such numbers possible, allowing enumeration of all active cells in the biological nitrogen-fixing community to become routine.

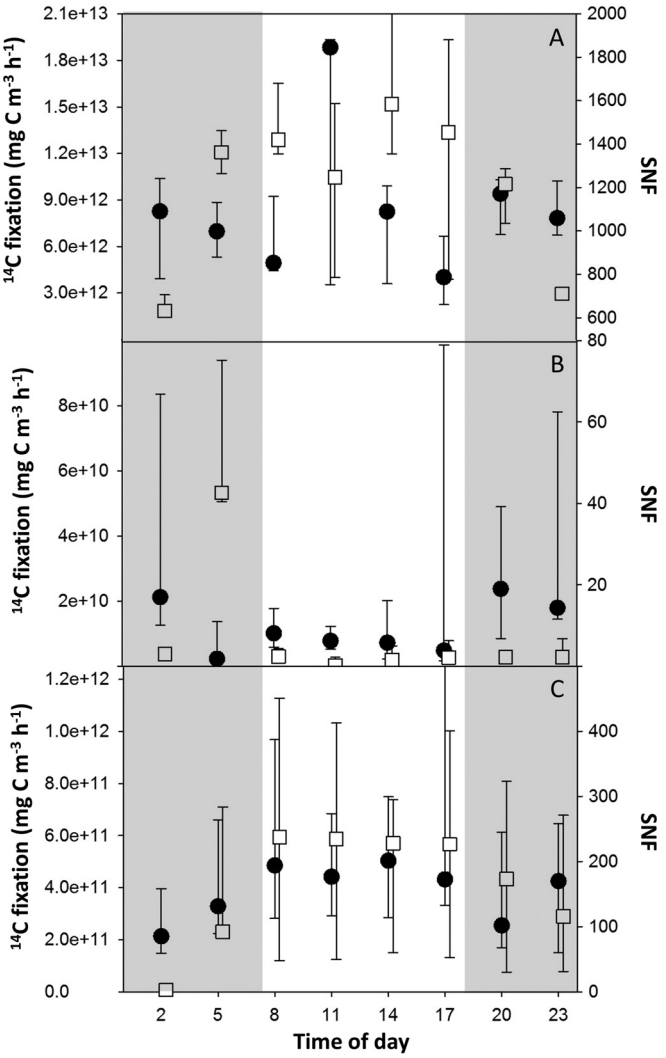

FIG 2 Diel cycle of size-normalized fluorescence (SNF; black circles) or primary production using ^{14}C P_{max} (white boxes) from triplicate laboratory samples. (A) *Synechococcus* sp.; (B) *Thoracosphaera heimii*; (C) *Thalassiosira oceanica*. Symbols represent median values from replicate samples. The top bar is the 75th percentile, and the bottom bar is the 25th percentile. Note the different strategies: *rbcL* mRNA expression leads C uptake in *Synechococcus* cultures, follows it closely with *T. oceanica*, and occurs at night in *T. heimii*.

Expression and rates. (i) Carbon fixation. From the photosynthesis versus irradiance curves prepared using the cultures of *Synechococcus* sp., *T. heimii*, and *T. oceanica* grown over a diel cycle (Fig. 2), we calculated P_{max}, the maximum ^{14}C uptake at saturating photon flux intensities, and differential gene expression using TSA-FISH (Fig. 3). The highest P_{max} in *Synechococcus* sp. was observed after the peak in *rbcL* transcription (Fig. 2A). *T. heimii* transcribed *rbcL* to a greater extent throughout the night than during the day (Fig. 2B). P_{max} rates were 10 times lower during the day (~4 mg C m^{-3} h^{-1}) than the highest rates at night (~45 mg C m^{-3} h^{-1}); peaks during the dark period are not unusual (54). *T. oceanica rbcL* expression and P_{max} were tightly coupled throughout the light and dark cycles (Fig. 2C), with maxi-

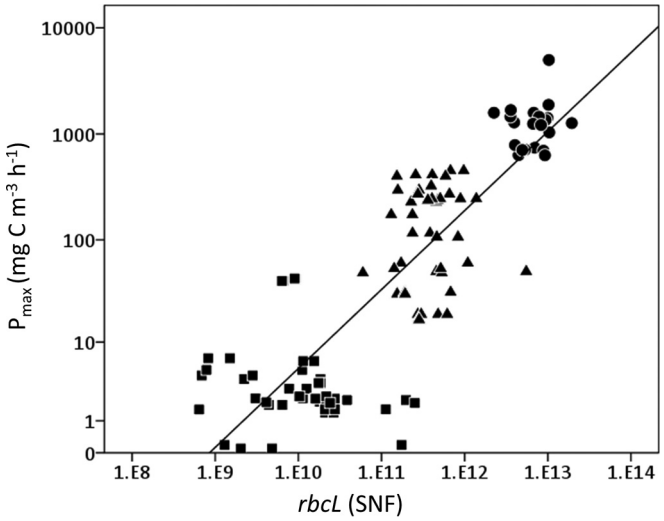

FIG 3 Regression of size-normalized fluorescence and C fixation. C fixation follows *rbcL* expression by 6 h; therefore, the determination of the relationship between C fixation and *rbcL* expression has been shifted 6 h. Measurements of the different cultures are represented using different symbols (circles, *Synechococcus* sp.; triangles, *T. oceanica*; squares, *T. heimii*). The regression line (center line) shows a strong correlation between size-normalized fluorescence and P_{max} and can be used to calculate C fixation from size-normalized fluorescence.

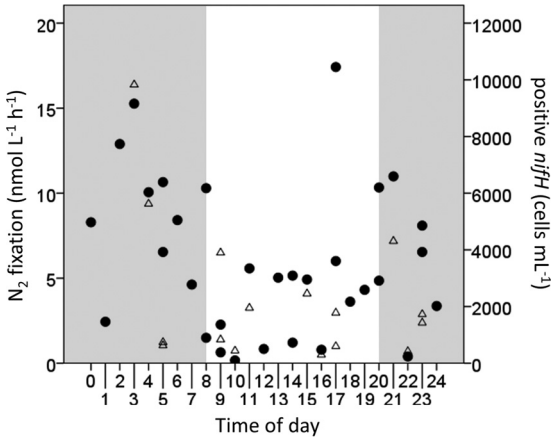

FIG 4 Environmental diel *nifH* expression and N fixation. Note the strong diel cycle of increased expression and N_2 fixation during dark hours and decreased expression and measured fixation during daylight hours. Circles represent the concentration of cells expressing *nifH* (cells ml^{-1}), and triangles represent N_2 fixation (nmol liter^{-1} h^{-1}).

mum values measured during the day and lowest values measured during the night (24). The greatest diatom P_{max} (~220 mg C m^{-3} h^{-1}) was five times higher than those measured in *T. heimii* but significantly lower than those measured in *Synechococcus* sp.

Marine primary producers range from prokaryotes to eukaryotes and span a size range covering many orders of magnitude (23). In order for samples covering a diverse range of cell types and sizes to be compared, the size-normalized fluorescence (SNF) was calculated for each of the cultures, removing fluorescent variability inherently associated with cell size, using the following equation:

$$\text{SNF} = ([\text{Fluoro}_{\text{sample}}/\text{Fluoro}_{\text{beads}}] \times [\text{FS}_{\text{sample}}/\text{FS}_{\text{beads}}]) \times \text{positive cells ml}^{-1} \quad (1)$$

Where $\text{Fluoro}_{\text{sample}}$ and $\text{Fluoro}_{\text{beads}}$ are the voltage values of red fluorescence for the respective particles and FS is the forward scatter of the particles (indicative of size).

Multiple-regression models then were used to determine correlation between *rbcL* expression (number of positive cells ml^{-1}) and P_{max} (maximum ^{14}C uptake) plus and minus a 3-, 6-, 9-, and 12-h time shift. We found *rbcL* expression lead P_{max} across the diel light cycle by 6 h ($r = 0.823$; $P < 0.001$) (Fig. 2); previous studies have shown strong correlations (3, 25, 27, 55) and that mRNA expression can lead P_{max} by 3 to 9 h (54). For *Synechococcus* sp. there was a maximum correlation between mRNA expression and P_{max} when P_{max} was shifted 6 h earlier ($F = 3.139$; $P = 0.093$; $n = 18$). Due to the consistency in cell size of *Synechococcus* sp., the size-normalized fluorescence measure may confound the relationship between mRNA expression and photosynthesis. That is, when ^{14}C uptake and SNF were compared there was no relationship, but when the *rbcL*-positive cell concentration is compared to the P_{max} ($F = 4.911$; $P = 0.04$; $n = 18$), the relationship was significant. In contrast, regression models show maximum correlation between mRNA expression (SNF) and P_{max} when P_{max} is shifted 6 h earlier ($F = 18.994$; $P < 0.001$; $n = 38$) for *T. heimii* (Fig. 2B). *T. oceanica* regression models show maximum correlation between mRNA expression (SNF) and P_{max} when there is no shift ($F = 2.195$; $P = 0.0147$; $n = 39$).

Measurement of rates using traditional methods (P_{max}) and mRNA FISH showed significant correlation (Fig. 3), allowing the determination of C fixation rates from size-normalized fluorescence using the equation of the regression line:

$$P_f = (3 \times 10^{-8}) \times (\text{SNF}/\mu\text{l})^{0.82} \quad (2)$$

The strength of the relationship ($r = 0.823$; $P < 0.001$) (Fig. 3) shows that it is possible not only to enumerate the cells ml^{-1} actively transcribing *rbcL*, accounting for differential expression between different components of the community (prokaryotes versus eukaryotes), but also to estimate C fixation.

Comparison of results of P_f (generated using TSA-FISH) and C fixation rates previously reported for the southeastern Indian Ocean are very similar. Estimated C fixation rates (P_f) from samples collected in the eastern Indian Ocean range from 0.2 to 8 mg C m^{-3} day^{-1} with a mean of 1.95 mg C m^{-3} day^{-1}, corresponding to rates previously reported for this region (56, 57). One station (which showed evidence of two size-differentiated groups of diazotrophs; see Fig. S6 in the supplemental material) had anomalously high values, ranging from 4.5 to 8.5 mg C m^{-3} day^{-1} through the diel cycle. When this station is removed, the values for the other 7 stations have a maximum value of 2.7 and an average of 1.36 mg C m^{-3} day^{-1}.

(ii) Nitrogen fixation. The highest positive *nifH* community expression, at stations sampled in the Indian ocean, was 10,500 cells ml^{-1} (19% of the total community), with an average of 600 cells ml^{-1} (7% of the total community), while the highest biological nitrogen fixation (BNF) rates were 16.38 nmol liter^{-1} h^{-1} (mean, 3.85 nmol liter^{-1} h^{-1}). The pattern observed in the eastern Indian Ocean (Fig. 4) mimics that of free-living single-celled diazotrophs (*Cyanothece* sp.) (42). This includes a peak in *nifH* expression (left *y* axis) and N_2 fixation (right *y* axis) at night and lowest values for both during the day. A regression model shows

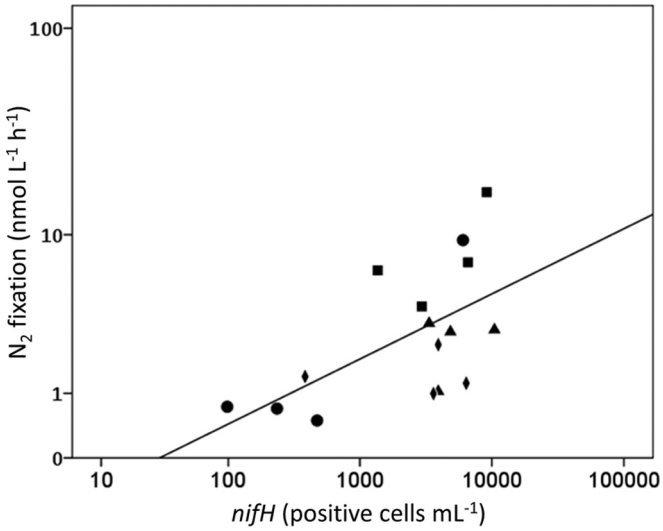

FIG 5 Regression of *nifH* expression versus biological nitrogen fixation in the eastern Indian Ocean. The different 24-h stations are represented by the different shapes (CTD16, triangles; D6, square; D27, diamonds; D48, circles; station locations can be found in Fig. S1 in the supplemental material). The regression line (center line) shows a strong correlation between positive target cells and N_2 fixation measured using traditional incubation methods and can be used to calculate N_2 fixation from positively tagged cells ml^{-1}.

significant correlation between mRNA-positive cells ml^{-1} measured at the start of incubations with measured $^{15}N_2$ uptake ($F = 6.194$; $P = 0.026$; $n = 16$).

Nitrogen fixing organisms are less diverse and span a smaller size range (52), though some are symbiotic with larger algae (58, 59). Changes in the fluorescence intensity of a sample then may be due more to positive target concentration than to differential expression (see equation 3). Therefore, the concentration of active *nifH* cells per ml was calculated and showed significant correlation (without any time shifts) with $^{15}N_2$ uptake ($r = 0.554$; $P = 0.026$) (Fig. 5) when examined for stations D6, D27, D48, and CTD16 (see Fig. S1 in the supplemental material) from the southeastern Indian Ocean. The resultant regression (Fig. 5, center line) can be used to estimate BNF from the number of *nifH*-positive cells in a sample:

$$\text{BNF} = (0.05) \times (\text{positive cells/ml})^{0.5} \quad (3)$$

Using the above-described equation to estimate BNF, rates range from 0.5 to 5 nmol $liter^{-1}$ h^{-1}, with an average value of 2.76 nmol $liter^{-1}$ h^{-1}, similar to those measured in this region (mean of 3.5 nmol $liter^{-1}$ h^{-1}) (41).

DISCUSSION

Cultured and environmental microbial populations actively transcribing *rbcL* and *nifH* were successfully hybridized using the method described and optimized in this study. Simultaneous measurements using traditional, direct measurements of isotopic C and N incorporation were significantly correlated with fluorescently labeled cells ($r^2 = 0.68$ and 0.45, respectively, as shown in Fig. 3 and 5, respectively). Our method not only yields number of cells actively fixing C and N but also can be used to estimate rates, providing a new approach for elucidating the connectivity of the C and N cycles simultaneously and on the same sample.

Using the various controls described in optimizing this method, the probes and optimization outlined here represents a reliable tool to quantify the active primary production and biological nitrogen fixation communities in environmental samples. These findings indicate the *rbcL* and *nifH* oligonucleotide probes are specific enough to detect the targeted processes (primary production and nitrogen fixation) in oligotrophic waters but are not so overly specific as to lead to nonspecific binding (e.g., in coastal waters where nitrogen fixation does not occur or in *E. coli* cultures that do not express either of these genes). Under the optimized conditions described, the increase in fluorescence above the background level allowed the differentiation of mRNA targets.

With the rapid advance of molecular work, including sequencing and RNA quantification, it would be advantageous for researchers utilizing this method to check the probe sequences against the vastly increasing diversity outlined in the repositories available (ours were aligned in January 2010). Care was taken in compiling multiple sequences from single and multiple species covering the diverse evolutionary histories of microbes targeted with these probes. Further, the probes and method (formamide concentration) were optimized to include variation in target sequences (using variable bases and lower hybridization temperatures). The parity in percentages of FISH-tagged microbes and measured percentages using flow cytometry (targeting groups using pigments and SYBR green) suggests that the majority of the population targeted was hybridized using the probes outlined here.

The importance of incorporation of diel periodicity into studies has been demonstrated previously in cultured phytoplankton, including representatives of diatoms, dinoflagellates, chlorophytes, chrysophytes, cyanobacteria (60), and environmental samples (19). This variation is similarly important when employing this method due to the lag between expression and fixation for both carbon and nitrogen. Diel variability, expressed as the amplitude of the cycle, ranges from 4 to 6 in environmental samples (19, 60, 61). Similar amplitudes in periodicity are demonstrated here: *Synechococcus* sp. strain 2-6 (mean, 4), *T. heimii* 3-29 (mean, 13), and *T. oceanica* 2-15 (mean, 6.5). Typical protocols for primary production measurements (i.e., incubations measuring the uptake of isotopically labeled C) suggest incubating through the light cycle (44). Integrated values of C fixation (P_{max}) for the entire diel cycle in this study are nearly two times higher than values integrated for the light period alone: ~46% less for *Synechococcus* sp., ~60% less for *T. heimii*, and ~44% less for *T. ocean*, similar to values previously reported (19, 61). Both the diel variability and potential underestimation of C fixation are greatest for *T. heimii*. Interestingly, the variability is lowest for *Synechococcus* sp. Correspondingly, rate measurements are overestimated when measurements only occur in the daylight for *Synechococcus* sp. and *T. oceanica*. *T. heimii* rates are underestimated, as the peak in carbon fixation occurs at night. Phytoplankton community composition likely plays an important role in variability in the diel cycle, as demonstrated by the different diel patterns presented here.

The work described here also presents insight into the diel cycles of both carbon and nitrogen fixation. Diatoms exhibit classical transcription and C fixation; both peak during the day. However, cyanobacteria can fix large amounts of C at night. At first this seems counterintuitive for photosynthesis, but actual fixation of C through action by RuBisCO is part of the dark reactions, which do not require light. Further, the dinoflagellates appear to have a different strategy altogether, with a large spike in C fixation just

prior to the start of the light cycle. These results indicate that (i) primary producer community composition is important in the determination of net primary production and (ii) a substantial portion of C fixation occurs at night. *Synechococcus* sp. and *Prochlorococcus* sp. dominate the open ocean environments (62). Thus, current estimates (63) and methods (1) of net primary production which extrapolate primary production contingent upon daylight hours may be underestimating the large amount of C fixation occurring in the dark.

There is no significant time lag between *nifH* transcription and BNF (Fig. 4). BNF and *nifH* expression peaked at night and were minimal during the daylight hours, temporally separating C and N fixation in natural populations. Such temporal separation of C and N fixation has been observed in laboratory samples (42). The observation of this pattern in environmental samples is particularly interesting because it points to the possibility that the N_2 fixation of the single-celled diazotrophic community (a large percentage of the microbial population in the southeastern Indian Ocean) in environmental samples is being temporally separated on an organismal level or that the O_2 generation (resulting from C fixation) on a community level inhibits N_2 fixation at the community level. Either scenario demonstrates the need to measure the interconnectivity of these two cycles on a fine temporal scale using the same methods.

The probes and optimization parameters outlined in this study provide an exciting new tool for elucidating the connectivity of the C and N cycles via simultaneous quantification of the fraction of the microbial community actively fixing C and N. Carbon fixation and biological nitrogen fixation are partially controlled by transcription of *rbcL* and *nifH* genes (24, 25, 27, 55). Therefore, mRNA TSA-FISH may offer new insights into the number of organisms actively performing these functions as well as estimates of these two processes. Instead of highly stringent, species-specific conditions, we also show it is possible to detect and quantify a more evolutionarily diverse, yet functionally similar, community. The power of quantifying functional gene expression *in situ* combines community enumeration and the estimation of important rate measurements. Flow cytometry allows more rapid quantification of positive cells than traditional epifluorescence microscopy, as well as the analysis of a larger number of events, thereby providing rapid, robust data sets. By combining detection of mRNA, using TSA-FISH, and enumeration via flow cytometry, the method optimized and outlined in this study offers robust, high-sensitivity analyses of active microbial populations.

ACKNOWLEDGMENTS

We thank John Norman (Beckman Coulter), who was extremely helpful in setting up and trouble-shooting the flow cytometer. Critiques from George A. Jackson, Anya Schulze, and Gilbert T. Rowe on early versions of the manuscript, as well as comments of three reviewers and the editor, improved the final version of the manuscript. We also thank Mona Hochman of the Seafood Safety Lab for providing negative-control cultures.

We acknowledge the facilities and scientific and technical assistance of the National Imaging Facility at the Centre for Microscopy, Characterization & Analysis, The University of Western Australia, a facility funded by the University, State, and Commonwealth Governments.

A.S.M. was supported by the NSF East Asia and Pacific Summer Institute Fellowship in conjunction with the Australian Academy of Science (grant number 1209422) during the initial phase of this work and later by a Texas A&M University Dissertation Fellowship. A.K.S. was supported by a Texas Sea Grant award to A.Q. The Australian phase of this work was supported by an ARC Discovery Grant to A.M.W. and coworkers. Indian Ocean ship time was awarded by the Australian Marine National Facility to Helen Phillips (University of Tasmania) and Chris Wilcox (CSIRO).

REFERENCES

1. **Behrenfeld MJ, Falkowski PG.** 1997. Photosynthetic rates derived from satellite-based chlorophyll concentration. Limnol. Oceanogr. **42:**1–20. http://dx.doi.org/10.4319/lo.1997.42.1.0001.
2. **Sabine CL, Feely RA, Gruber N, Key RM, Lee K, Bullister JL, Wanninkhof R, Wong CS, Wallace DWR, Tilbrook B, Millero FJ, Peng T-H, Kozyr A, Ono T, Rios AF.** 2004. The oceanic sink for anthropogenic CO_2. Science **305:**367–371. http://dx.doi.org/10.1126/science.1097403.
3. **Chassot E, Bonhommeau S, Dulvy NK, Melin F, Watson R, Gascuel D, Le Pape O.** 2010. Global marine primary production constrains fisheries catches. Ecol. Lett. **13:**495–505. http://dx.doi.org/10.1111/j.1461-0248.2010.01443.x.
4. **Dugdale RC, Goering JJ.** 1967. Uptake of new and regenerated forms of nitrogen in primary productivity. Limnol. Oceanogr. **12:**196–206. http://dx.doi.org/10.4319/lo.1967.12.2.0196.
5. **Fawcett SE, Lomas MW, Casey JR, Ward BB, Sigman DM.** 2011. Assimilation of upwelled nitrate by small eukaryotes in the Sargasso Sea. Nat. Geosci. **4:**717–722. http://dx.doi.org/10.1038/ngeo1265.
6. **Gruber N.** 2005. A bigger nitrogen fix. Nature **436:**786–787. http://dx.doi.org/10.1038/436786a.
7. **Gruber N.** 2008. The marine nitrogen cycle: overview and challenges, p 1–50. *In* Capone DG, Bronk DA, Mulholland MR, Carpenter EJ (ed), Nitrogen in the marine environment. Elsevier, Amsterdam, The Netherlands.
8. **Eppley RW, Peterson BJ.** 1979. Particulate organic matter flux and planktonic new production in the deep ocean. Nature **282:**677–680. http://dx.doi.org/10.1038/282677a0.
9. **Jeffrey SW, Mantoura RFC, Wright SW.** 1997. Phytoplankton pigments in oceanography, guidelines to modern methods, vol 10. UNESCO, Paris, France.
10. **Lomas MW, Bronk D, van den Engh AG.** 2011. Use of flow cytometry to measure biogeochemical rates and processes in the ocean. Annu. Rev. Mar. Science **3:**537–566. http://dx.doi.org/10.1146/annurev-marine-120709-142834.
11. **Marie D, Partensky F, Jacquet S, Vaulot D.** 1997. Enumeration and cell cycle analysis of natural populations of marine picoplankton by flow cytometry using the nucleic acid stain SYBR green I. Appl. Environ. Microbiol. **63:**186–193.
12. **Gran HH, Gaarder T.** 1927. Investigations of the production of plankton in the Oslo Fjord. Conseil Permanent International pour L'Exploration de la Mer.
13. **Yallop ML.** 1982. Some effects of light on algal respiration and the validity of the light and dark bottle technique for measuring primary productivity. Freshw. Biol. **12:**427–433.
14. **Steeman-Nielsen E.** 1953. Use of radioactive carbon (C^{14}) for measuring organic production in the sea. J. Cons. Int. Explor. Mer. **18:**117–140.
15. **Bender M, Grande K, Johnson K, Marra J, Williams PJL, Seiburth J, Pilson M, Langdon C, Hitchcock G, Orchardo J, Hunt C, Donaghay P, Heinemann K.** 1987. A comparison of four methods for determining planktonic community production. Limnol. Oceanogr. **32:**1085–1098. http://dx.doi.org/10.4319/lo.1987.32.5.1085.
16. **Luz B, Barkan E.** 2000. Assessment of oceanic productivity with the triple-isotope composition of dissolved oxygen. Science **288:**2028–2031. http://dx.doi.org/10.1126/science.288.5473.2028.
17. **Kolber ZS, Falkowski PG.** 1993. Use of active fluorescence to estimate phytoplankton photosynthesis *in situ*. Limnol. Oceanogr. **38:**1646–1665. http://dx.doi.org/10.4319/lo.1993.38.8.1646.
18. **Kolber ZS, Prášil O, Falkowski PG.** 1998. Measurements of variable chlorophyll fluorescence using fast repetition rate techniques: defining methodology and experimental protocols. Biochim. Biophys. Acta **1367:**88–106. http://dx.doi.org/10.1016/S0005-2728(98)00135-2.
19. **Harding LW, Jr, Prezelin BB, Sweeney BM, Cox JL.** 1982. Primary production as influenced by diel periodicity of phytoplankton photosynthesis. Mar. Biol. **67:**179–186. http://dx.doi.org/10.1007/BF00401283.
20. **Mohr W, Groβkopf T, Wallace DWR, LaRoache J.** 2010. Methodological underestimation of oceanic nitrogen fixation rates. PLoS One **5:**1–7. http://dx.doi.org/10.1371/journal.pone.0012583.
21. **Montoya JP, Voss M, Kahler P, Capone D.** 1996. A simple, high-

precision, high-sensitivity tracer assay for N_2 fixation. Appl. Environ. Microbiol. **62:**986–993.
22. **Neess JC, Dugdale RC, Dugdale VA, Goering JJ.** 1962. Nitrogen metabolism in lakes. I. Measurement of nitrogen fixation with N^{15}. Limnol. Oceanogr. **7:**163–169.
23. **Kirchman DL.** 2008. Microbial ecology of the oceans, 2nd ed. John Wiley & Sons, Inc., New York, NY.
24. **Corredor JE, Wawrik B, Paul JH, Tran H, Kerkhof L, Lopez JM, Dieppa A, Cardenas O.** 2004. Geochemical rate-RNA integration study: ribulose-1,5-bisphosphate carboxylase/oxygenase gene transcription and photosynthetic capacity of planktonic photoautotrophs. Appl. Environ. Microbiol. **70:**5459–5468. http://dx.doi.org/10.1128/AEM.70.9.5459-5468.2004.
25. **John DE, Wang ZA, Liu X, Byrne RH, Corredor JE, Lopez JM, Cabrera A, Bronk DA, Tabita FR, Paul JH.** 2007. Phytoplankton carbon fixation gene (RuBisCO) transcripts and air-sea CO_2 flux in the Mississippi River plume. ISME J. **1:**517–531. http://dx.doi.org/10.1038/ismej.2007.70.
26. **Pernthaler A, Amann R.** 2004. Simultaneous fluorescence *in situ* hybridization of mRNA and rRNA in environmental bacteria. Appl. Environ. Microbiol. **70:**5426–5433. http://dx.doi.org/10.1128/AEM.70.9.5426-5433.2004.
27. **Martin-Nieto J, Herrero A, Flores E.** 1991. Control of nitrogenase mRNA levels by products of nitrate assimilation in the cyanobacterium *Anabena* sp. strain PCC 7120. Plant Physiol. **97:**825–828. http://dx.doi.org/10.1104/pp.97.2.825.
28. **Pilhofer M, Pavlekovic M, Lee NM, Ludwig W, Schleifer K-H.** 2009. Fluorescence *in situ* hybridization for intracellular localization of *nifH* mRNA. Syst. Appl. Microbiol. **32:**186–192. http://dx.doi.org/10.1016/j.syapm.2008.12.007.
29. **Lee JHW, Katano T, Chang M, Han M-S.** 2012. Application of tyramide signal amplification-fluorescence in situ hybridization and flow cytometry to detection of *Heterosigma akashiwo* (Raphidophyceae) in natural waters. N. Z. J. Mar. Freshw. Res. **46:**137–148. http://dx.doi.org/10.1080/00288330.2011.613404.
30. **Lefort T, Gasol JM.** 2013. Global-scale distributions of marine surface bacterioplankton groups along gradients of salinity, temperature, and chlorophyll: a meta-analysis of fluorescence *in situ* hybridization studies. Aquat. Microb. Ecol. **70:**111–130. http://dx.doi.org/10.3354/ame01643.
31. **Pernthaler J, Glockner FO, Schonhuber W, Amann R.** 2001. Fluorescence *in situ* hybridization, p 211–226. *In* Paul J (ed), Marine microbiology, vol 30. Academic Press Ltd., London, United Kingdom.
32. **Prichard SL, Campbell L, Carder KL, Kang JB, Patch J, Tabita FR, Paul JH.** 1997. Analysis of ribulose bisphosphate carboxylase gene expression in natural phytoplankton communities by group-specific gene probing. Mar. Ecol. Prog. Ser. **149:**239–253. http://dx.doi.org/10.3354/meps149239.
33. **Pernthaler A, Pernthaler J, Amann R.** 2004. Sensitive multi-color fluorescence *in situ* hybridization for the identification of environmental microorganisms, p 711–726. *In* Molecular microbial ecology manual, vol 3. Kluwer Academic Publishers, Dordrecht, Netherlands.
34. **Yan F, Wu X, Crawford M, Duan W, Wilding EE, Gao L, Nana-Sinkam SP, Villalona-Calero MA, Baiocchi RA, Otterson GA.** 2010. The search for an optimal DNA, RNA, and protein detection by *in situ* hybridization, immunohistochemistry, and solution-based methods. Methods **52:**281–286. http://dx.doi.org/10.1016/j.ymeth.2010.09.005.
35. **Raes EJ, Waite AM, McInnes AS, Olsen H, Nguyen HM, Hardman-Mountford N, Thompson PA.** Changes in latitude and dominant diazotrophic community alter N_2 fixation. Mar. Ecol. Prog. Ser., in press.
36. **Zehr JP, Jenkins BD, Short SM, Steward GF.** 2003. Nitrogenase gene diversity and microbial community structure: a cross-system comparison. Environ. Microbiol. **5:**539–554. http://dx.doi.org/10.1046/j.1462-2920.2003.00451.x.
37. **Wallner G, Amann R, Beisker W.** 1993. Optimizing fluorescent *in situ* hybridization with rRNA-targeted oligonucleotide probes for flow cytometric identification of microorganisms. Cytometry **14:**136–143. http://dx.doi.org/10.1002/cyto.990140205.
38. **van de Corput MPC, Dirks RW, van Gijlswijk RPM, van Binnendijk E, Hattinger CM, de Paus RA, Landegent JE, Raap AK.** 1998. Sensitive mRNA detection by fluorescence *in situ* hybridization using horseradish peroxidase-labelled oligonucleotides and tyramide signal amplification. J. Histochem. Cytochem. **46:**1249–1259. http://dx.doi.org/10.1177/002215549804601105.
39. **Guillard R, Ryther J.** 1962. Studies of marine planktonic diatoms. I. Cyclotella nana Hustedt, and *Detonula confervacea* (cleve) Gran. Can. J. Microbiol. **8:**229–239.
40. **Dorado S, Rooker JR, Wissel B, Quigg A.** 2012. Isotope baseline shifts in pelagic food webs of the Gulf of Mexico. Mar. Ecol. Prog. Ser. **464:**37–49. http://dx.doi.org/10.3354/meps09854.
41. **Sekar R, Fuchs BM, Amann R, Pernthaler J.** 2004. Flow sorting of marine bacterioplankton after fluorescence *in situ* hybridization. Appl. Environ. Microbiol. **70:**6210–6219. http://dx.doi.org/10.1128/AEM.70.10.6210-6219.2004.
42. **Berman-Frank I, Quigg A, Finkel ZV, Irwin AJ, Haramaty L.** 2007. Nitrogen-fixation strategies and Fe requirements in cyanobacteria. Limnol. Oceanogr. **52:**2260–2269. http://dx.doi.org/10.4319/lo.2007.52.5.2260.
43. **Lewis MR, Smith JC.** 1983. A small volume, short-incubation-time method for measurement of photosynthesis as a function of incident irradiance. Mar. Ecol. Prog. Ser. **13:**99–102. http://dx.doi.org/10.3354/meps013099.
44. **Knap A, Michaels A, Close A, Ducklow H, Dickson A.** 1996. Protocols for the Joint Global Ocean Flux Study (JGOFS) core measurements. JGOFS report 19. US JGOFS, Woods Hole, MA.
45. **Großkopf T, Mohr W, Baustian T, Schunck H, Gill D, Kuypers MMM, Lavik G, Schmitz RA, Wallace DWR, LaRoache J.** 2012. Doubling of marine dinitrogen-fixation rates based on direct measurements. Nature **488:**361–364. http://dx.doi.org/10.1038/nature11338.
46. **Chen Y-B, Zehr JP, Mellon M.** 1996. Growth and nitrogen fixation of the diazotrophic filamentous nonheterocystous cyanobacterium *Trichodesmium* sp. IMS101 in defined media: evidence for a circadian rhythm. J. Phycol. **32:**916–932.
47. **Hougaard DM, Hansen H, Larsson L-I.** 1997. Non-radioactive *in situ* hybridization for mRNA with emphasis on the use of oligodeoxynucleotide probes. Histochem. Cell Biol. **108:**335–344. http://dx.doi.org/10.1007/s004180050174.
48. **Hyka P, Lickova S, Pribyl P, Melzoch K, Kovar K.** 2012. Flow cytometry for the development of biotechnological processes with microalgae. Biotechnol. Adv. **31:**2–16. http://dx.doi.org/10.1016/j.biotechadv.2012.04.007.
49. **Biegala IC, Not F, Vaulot D, Simon N.** 2003. Quantitative assessment of picoeukaryotes in the natural environment by using taxon-specific oligonucleotide probes in association with tyramide signal amplification-fluorescence *in situ* hybridization and flow cytometry. Appl. Environ. Microbiol. **69:**5519–5529. http://dx.doi.org/10.1128/AEM.69.9.5519-5529.2003.
50. **Wawrik B, Paul JH, Tabita FR.** 2002. Real-time PCR quantification of *rbcL* (ribulose-1,5-bisphosphate carboxylase/oxygenase) mRNA in diatoms and pelagophytes. Appl. Environ. Microbiol. **68:**3771–3779. http://dx.doi.org/10.1128/AEM.68.8.3771-3779.2002.
51. **Wyman M.** 1999. Diel rhythms in ribulose-1,5-bisphosphate carboxylase/oxygenase and glutamine synthetase gene expression in a natural population of marine picoplanktonic cyanobacteria (*Synechococcus* spp.). Appl. Environ. Microbiol. **65:**3651–3659.
52. **Church MJ, Jenkins BD, Karl DM, Zehr JP.** 2005. Vertical distributions of nitrogen-fixing phylotypes at Stn ALOHA in the oligotrophic north Pacific Ocean. Aquat. Microb. Ecol. **38:**3–14. http://dx.doi.org/10.3354/ame038003.
53. **Zehr JP, Waterbury JB, Turner PJ, Montoya JP, Omoregie E, Steward GF, Hansen A, Karl DM.** 2001. Unicellular cyanobacteria fix N_2 in the subtropical north Pacific ocean. Nature **412:**635–638. http://dx.doi.org/10.1038/35088063.
54. **John DE, Lopez-Diaz JM, Cabrera A, Santiago NA.** 2012. A day in the life in the dynamic marine environment: how nutrients shape diel patterns of phytoplankton photosynthesis and carbon fixation gene expression in the Mississippi and Orinoco River plumes. Hydrobiologia **679:**155–173. http://dx.doi.org/10.1007/s10750-011-0862-6.
55. **Paul JH, Kang JB, Tabita FR.** 2000. Diel patterns of regulation of *rbcL* transcription in a cyanobacterium and a prymnesiophyte. Mar. Biotechnol. **2:**429–436.
56. **Holl CM, Villareal TA, Payne CD, Clayton TD, Hart C, Montoya JP.** 2007. *Trichodesmium* in the western gulf of Mexico: $^{15}N_2$-fixation and natural abundance stable isotope evidence. Limnol. Oceanogr. **52:**2249–2259. http://dx.doi.org/10.4319/lo.2007.52.5.2249.
57. **Waite AM, Pesant S, Griffin DA, Thompson PA, Holl CM.** 2007. Oceanography, primary production and dissolved inorganic nitrogen uptake in two Leeuwin Current eddies. Deep Sea Res. 2 Top. Stud. Oceanogr. **54:**981–1002. http://dx.doi.org/10.1016/j.dsr2.2007.03.001.

58. **Carpenter EJ, Montoya JP, Burns J, Mulholland MR, Subramaniam A, Capone DG.** 1999. Extensive bloom of a N_2-fixing diatom/cyanobacterial association in the tropical Atlantic Ocean. Mar. Ecol. Prog. Ser. **185:**273–283. http://dx.doi.org/10.3354/meps185273.
59. **Zehr JP, Carpenter EJ, Villareal TA.** 2000. New perspectives on nitrogen-fixing microorganisms in tropical and subtropical oceans. Trends Microbiol. **8:**68–73. http://dx.doi.org/10.1016/S0966-842X(99)01670-4.
60. **Harding LW, Jr, Meeson BW, Prezelin BB, Sweeney BM.** 1981. Diel periodicity of photosynthesis in marine phytoplankton. Mar. Biol. **61:**95–105. http://dx.doi.org/10.1007/BF00386649.
61. **Yoshikawa T, Furuya K.** 2006. Effects of diurnal variations in phytoplankton photosynthesis obtained from natural fluorescence. Mar. Biol. **150:**299–311. http://dx.doi.org/10.1007/s00227-006-0331-3.
62. **Paul JH.** 1996. Carbon cycling: molecular regulation of photosynthetic carbon fixation. Microb. Ecol. **32:**231–245.
63. **Field CB, Behrenfeld MJ, Randerson JT, Falkowski P.** 1998. Primary production of the biosphere: integrating terrestrial and oceanic components. Science **281:**237–240. http://dx.doi.org/10.1126/science.281.5374.237.
64. **Falkowski PG, Laws EA, Barber RT, Murray JW.** 2003. Phytoplankton and their role in primary, new and export production, p 99–121. *In* Fasham MJR (ed), Ocean biogeochemistry the role of the ocean carbon cycle in global change. Springer-Verlag, Berlin, Germany.
65. **Hardy RWF, Holsten RD, Jackson EK, Burns RC.** 1968. The acetylene-ethylene assay for N_2 fixation: laboratory and field evaluation. Plant Physiol. **43:**1185–1207. http://dx.doi.org/10.1104/pp.43.8.1185.